Milan Hokr

Benchmark calculations of the variable-density flow in porous media

In: Jan Chleboun and Karel Segeth and Tomáš Vejchodský (eds.): Programs and Algorithms of Numerical Mathematics, Proceedings of Seminar. Prague, May 28-31, 2006. Institute of Mathematics AS CR, Prague, 2006. pp. 104–110.

Persistent URL: http://dml.cz/dmlcz/702825

BENCHMARK CALCULATIONS OF THE VARIABLE-DENSITY FLOW IN POROUS MEDIA*

Milan Hokr

1. Introduction

Variable-density (or density-driven, density-dependent) porous media flow problem is a coupled problem of water flow and solute transport: the water velocity as a result of the flow problem is a parameter in the solute transport problem (standard case) and the solution density as a parameter in the flow problem is dependent on concentration, a result of the transport problem (specific for variable-density flow) [1].

Several standard benchmark problems are used for tests of numerical schemes and simulation codes [2, 1]; they are mostly derived from real-world problems of seawater intrusion and salt deposits. We propose a new benchmark problem, with a configuration derived from a case-study of groundwater flow and contaminant transport in the former uranium leaching site Stráž pod Ralskem in the north of the Czech Republic. The improvement is in parametrization of the intensity of the density coupling, allowing to study the efficiency of numerical schemes in dependence on physical parameters and also to find the limits for using simpler numerical schemes for the variable-density flow problem.

2. Governing equations

The groundwater porous media flow with the Boussinesque approximation [2] is governed by the Darcy's law and the mass-balance (continuity) equation

$$\boldsymbol{u} = (\boldsymbol{K}(\nabla h + \varrho_r \nabla z)), \qquad \kappa \frac{\partial h}{\partial t} - \nabla \cdot \boldsymbol{u} = q\,, \tag{1}$$

where h is the pressure head, ϱ_r is the relative solution density (with respect to the fresh water density), $\boldsymbol{u}$ is the Darcy velocity, q is the source/sink rate, $\boldsymbol{K}$ is the hydraulic conductivity tensor, κ is the storativity coefficient, and z is the vertical coordinate. The solute transport is governed by the advection-diffusion equation

$$\frac{\partial\,(nc)}{\partial t} + \nabla \cdot (\boldsymbol{u}c) - \nabla \cdot (n\boldsymbol{D}\nabla c) = qc_0\,, \tag{2}$$

*This work was supported with the subvention from the Grant Agency of the Czech Republic, project code 102/05/P284.

where c is the solute concentration, c_0 is a concentration in the source/sink, $\boldsymbol{D}$ is the hydrodynamic dispersion tensor [2], and n is the porosity.

The flow and transport equations are coupled through the Darcy velocity $\boldsymbol{u} = \boldsymbol{K}(\nabla h + \varrho_r \nabla z)$ and through the relative density, which is a function of the concentration, in the simplest case $\varrho_r(c) = 1 + c/\varrho_0$, where ϱ_0 is the fresh water density.

3. Numerical schemes

We use two schemes (MHFEM and CVFEM) denoted by the name of the method used for the flow problem. In both schemes, the advective transport problem is solved by principally same upwind finite volumes (the only difference is the position of the control volume – primal or dual mesh, see below). The hydrodynamic dispersion term is not evaluated in neither of the schemes. The main motivation for the choice of these numerical methods is the consistent discrete representation of velocity in both the flow and transport schemes, preserving the local mass balance. Both the methods use a discretization with trilateral prisms, which allow to use simpler mesh topology with the horizontal triangulation and the prisms ordered to layers and columns.

We use the computer codes (different for each method) developed before for general groundwater problems, with the variable-density term recently added. The codes have been successfully tested in several model and real-world problems.

3.1. Mixed-hybrid finite-element scheme

The MHFEM scheme is based on the weak formulation of the system of equations (1) on a system of elements $e \in \mathcal{E}_h$ with the additional constraint condition of mass balance expressed by Lagrange multipliers [5]. Thus, there are three unknown functions approximated with the following discrete spaces: the pressure head h by piecewise constant functions (in elements), the Lagrange multipliers (physically "pressure on inter-element interfaces") by piecewise constant functions on sides, and the velocity $\boldsymbol{u}$ by piecewise linear vector functions (lowest-order Raviart-Thomas space). The exact formulation for the specific case of trilateral prismatic elements is given in [5].

The approximation of the variable-density term results directly in the right-hand side of the weak formulation of the first equation of (1), i.e.

$$\sum_{e\in\mathcal{E}_h} \{(\boldsymbol{A}\boldsymbol{u}^e, \boldsymbol{v}^e)_{0,e} - (p^e, \nabla\cdot\boldsymbol{v}^e)_{0,e} + \langle \lambda^e, \boldsymbol{\nu}^e\cdot\boldsymbol{v}^e\rangle_{\partial e\cap\Gamma_h}\} \;=$$

$$\sum_{e\in\mathcal{E}_h} \{\langle p_D, \boldsymbol{\nu}^e\cdot\boldsymbol{v}^e\rangle_{\partial e\cap\partial\Omega_D} + \langle \varrho_r z, \boldsymbol{v}^e\cdot\boldsymbol{\nu}^e\rangle_{\partial e} - (\varrho_r z, \nabla\cdot\boldsymbol{v}^e)_{0,e}\}, \tag{3}$$

where $\boldsymbol{A} = \boldsymbol{K}^{-1}$, $\boldsymbol{v}$ are test functions from the same Raviart-Thomas space as $\boldsymbol{u}$, $\boldsymbol{\nu}$ is the outward normal vector, $(\cdot,\cdot)_{0,e}$ and $\langle\cdot,\cdot\rangle_{\partial e}$ are the L_2 scalar products on the element volume and the element boundary respectively, $\partial\Omega_D$ is the Dirichlet

boundary, and p_D is the boundary value of p. In the discrete form, the last two terms on the right-hand side are evaluated as a difference between the z coordinates of the mass centre of the element and the mass centre of the particular side. The time discretisation is implicit Euler, but in the calculations below we use a sequence of steady states with variable parameters, which corresponds to a very large value of the storativity κ.

The finite volume scheme for the transport problem is described in [3]; the cells are geometrically identical with the elements of MHFEM flow problem solution, we use the cell-centred approximation, the upwind weighting of the advective flux, and the explicit time discretisation. The MHFEM discrete unknowns of the velocity approximation are the fluxes through element sides, conservative with respect to the element volumes, which are directly the input value for the discrete advection term.

3.2. Control-volume finite-element scheme

The CVFEM scheme is based on a combination of two ideas: understanding the basic piecewise linear finite element solution with the triangular mesh as a finite volume scheme on the dual mesh (control volumes around the mesh nodes) and combining the FE scheme for 2D horizontal triangulation with the finite differences for the vertical discretization. This technique including the variable-density term in a mass-balance form is derived in [4].

The weak formulation, semidiscrete in the vertical direction, for a layer k is

$$(K^{xy}\nabla_{xy}h_k, \nabla_{xy}\phi_k)_{\Omega_k} - \left(\frac{1}{\Delta z_k}\left[K^z_{k+\frac{1}{2}}\frac{h_{k+1}-h_k}{\Delta z_{k+\frac{1}{2}}} - K^z_{k-\frac{1}{2}}\frac{h_k-h_{k-1}}{\Delta z_{k-\frac{1}{2}}}\right], \phi_k\right)_{\Omega_k} = (q_k, \phi_k)_{\Omega_k}, \tag{4}$$

where K^{xy} and K^z are components of $\boldsymbol{K}$ in the x, y directions and z direction respectively, ∇_{xy} is the ∇ operator in the xy direction, $\Delta z_{k+\frac{1}{2}}$ is the vertical discretisation step between the layers k and $k+1$, $(\cdot,\cdot)_{\Omega_k}$ is the L_2 scalar product in the layer k (horizontal projection of problem domain Ω), ϕ_k is a piecewise linear test function.

The pressures and the concentrations are evaluated in the mesh nodes, the velocity is represented as fluxes along mesh edges, the flux between nodes i and j is $u_{ij} = \mathbb{A}_{ij}(h_i - h_j)$, where $\mathbb{A}$ is the global stifness matrix, and h_i, h_j are the nodal values of pressure head.

3.3. Variable-density coupling

The model uses the explicit time stepping, i.e. in each time step, the flow problem is solved with the density distribution from the previous time step and then the transport problem is solved with the updated velocity field. This approach requires a small time step. The benchmark below is sensitive to change of the coupling time step in the beginning of the time interval, but the sufficient time step is still 10 times larger than the stability condition given by the upwind scheme for the solute transport. In the calculations, the time step is 40 days for the transport scheme and 360 days for the coupling iterations.

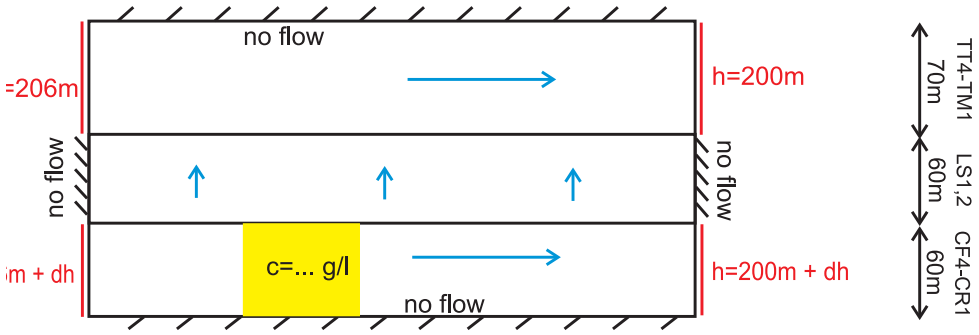

Fig. 1: *Configuration of the benchmark problem, position of boundary and initial conditions.*

Layer code	K_x, K_y	K_z	n	dz	$c_{ini}^{(10)}$	$c_{ini}^{(30)}$	$c_{ini}^{(50)}$
	m/day	m/day	1	m	g/l	g/l	g/l
TT4 – TT1	6 – 10	6 – 10	0.07	10–15	0	0	0
TM2 – TM1	0.4	0.1	0.07	12.5	0	0	0
LS2 – LS1	1e-4	4e-4	0.05	30	0	0	0
CF4 – CF3	0.5	0.25	0.08	12.5	10	25	40
CF2	0.05	0.025	0.04	7.5	10	20	30
CF1	0.5	0.25	0.08	7.5	10	25	40
CR2 – CR1	2 – 4	2	0.1	8–12	10	30	50

Tab. 1: *Discretization and material parameters in the benchmark: horizontal and vertical conductivity, porosity, layer thickness, and three variants of initial concentration. Some lines represent multiple layers with slightly variable parameters.*

4. Benchmark structure

4.1. Discretization and material parameters

The benchmark problem is built as geometrically simple domain representing the most of the character of the real groundwater system in Stráž pod Ralskem. The domain is 2000 m long (left–right), 190 m high and 40 m wide (front–back), discretized with prisms coupled in hexahedrons, each of the size $40 \times 40 \times dz$ (the thickness varies). The vertical discretisation is by 14 layers with thickness dz according to the real geological structure (Fig. 1, Tab. 1). We use the codes originated from the rock names: "T" the top permeable part (aquifer), "L" the semi-isolator, "C" the bottom part (aquifer).

4.2. Boundary conditions

The boundary conditions are Dirichlet (prescribed pressure head h) and homogeneous Neumann (zero flux $\boldsymbol{u} \cdot \boldsymbol{\nu} = 0$) for the flow problem (Fig. 1). The pressure head difference between the bottom and the top part is a parameter dh, representing

the intensity of the hydraulic force in comparison with the gravity force on denser liquid (larger dh means less density-dependent coupling), $dh = 1\,\mathrm{m}$, $3\,\mathrm{m}$, and $10\,\mathrm{m}$. For the solute advection problem, zero Dirichlet at the inflow boundary is prescribed (fresh water $c = 0$), no boundary condition is prescribed at the outflow boundary, and the position of zero flux boundaries is the same as for the flow problem.

4.3. Initial conditions

The initial distribution of head and velocity (flow problem) is given by the boundary conditions above (constant-density steady state). As the initial distribution of concentration (transport problem), we use a simple representation of a contamination plum in the bottom aquifer, with zero concentration elsewhere (Fig. 1).

The contamination plum is defined by constant concentration for each layer, with horizontal dimension (length) 280 m and position 200 m from the left, with vertical inhomogeneity given by field measurements. We use three variants (referred by the most bottom value) in Tab.1. They are the second parameter of density-coupling (the higher is the concentration, the more is the density influence).

5. Results

We observe the behaviour of the system in the time interval of 200 years. During this interval the contamination in the most permeable layers leaves the domain, but the slowly moving contamination in the less permeable layers moves to the central and the right part of the domain and the transfer upwards is well visible (Fig. 2).

The objective of the numerical benchmark study is to compare two different approximations (equations coupled/uncoupled), two different numerical schemes, and mesh refinement. The results are expressed by integral values of concentration over each layer of the discretization (total mass in a layer). This technique is kept from previous use of the benchmark for hydrogeological parametric studies.

5.1. Basic study of parameter influence

Table 2 compares the total transfer to the top aquifer for the combinations of the three values of the piezometric head difference dh and the three variants of initial contamination, calculated with MHFEM scheme. For each combination, we also compare the variable-density and the constant-density model formulation.

For the head difference $dh = 1\,\mathrm{m}$, the hydraulic force is small and the gravity force and the density-driven process dominate, so much that the mass transfer upwards partly decreases with rising concentration. For the head difference $dh = 3\,\mathrm{m}$ and $dh = 10\,\mathrm{m}$, the hydraulic force becomes more significant but the density effect keeps important. The smallest influence and the weakest coupling is as expected for $dh = 10\,\mathrm{m}$ and $c = 10\,\mathrm{g/l}$. The basic analysis in Tab. 2 documents the necessity of the variable-density model and a good sensitivity on the density approximation required for variable-density benchmarks.

Initial	$dh = 1$		$dh = 3$		$dh = 10$	
conc.	var.dens.	const.dens.	var.dens.	const.dens.	var.dens.	const.dens.
g/l	ton	ton	ton	ton	ton	ton
10	0.165	0.568	5.07	11.897	67.883	100.643
30	0.105	1.419	6.181	29.578	116.717	251.165
50	0.117	2.269	7.058	47.26	156.037	401.688

Tab. 2: *Evaluation of the parameter influence and comparison of the variable-density versus the constant-density approximation, by means of a single value of the total mass transfer to the upper aquifer (subdomain).*

	$dh = 1$ $c = 50$			$dh = 3$ $c = 30$			$dh = 10$ $c = 10$		
	orig	ref1	ref2	orig	ref1	ref2	orig	ref1	ref2
top	0.828	0.028	1E-04	6.645	1.091	0.184	75.55	66.72	48.11
isolator	33.46	14.13	3.579	62.04	31.01	13.58	105.2	138.7	88.78
bottom	167.1	141.2	57.82	120.4	125.1	56.9	24.58	52.45	54.23

Tab. 3: *Study of the mesh refinement in z direction, results expressed by three values of the total mass in the bottom, middle, and top part of the domain.*

5.2. Mesh refinement

We narrow the study to the following three combinations representing the weakest, medium and the strongest density coupling respectively: (a) $dh = 10\,\mathrm{m}$, $c = 10\,\mathrm{g/l}$, (b) $dh = 3\,\mathrm{m}$, $c = 30\,\mathrm{g/l}$, and (c) $dh = 1\,\mathrm{m}$, $c = 50\,\mathrm{g/l}$. The mesh is refined in the z direction, i.e. each layer in Tab. 1 is divided into two equal.

The results of CVFEM calculation[1] expressed as mass sums in each of the three parts are in Tab. 3. The density influence is similar in all the original and the refined meshes, but there is no visible convergence. Generally, finer mesh lead to smaller transfer to upper layers, which can be caused by smaller numerical diffusion. On the other hand, the overall trend visualised by concentration field is similar for all discretizations (Fig. 2). The difficulty for comparing the MHFEM and CVFEM schemes is in the different position of unknowns with respect to the material parameters in the layers. As examples of secondary importance, the three corresponding values in Tabs. 2 and 3 are less different than with respect to the mesh refinement.

6. Conclusion

The results confirm the great enough sensitivity of the defined benchmark on the variable-density coupling. Moreover, the chosen parameters well cover the interval between the weak and strong coupling.

[1]The refinements for MHFEM were not evaluated, because the code uses external solver of the system of linear algebraic equations, which leads to very slow calculation in the iterations. We currently work on a more efficient implementation.

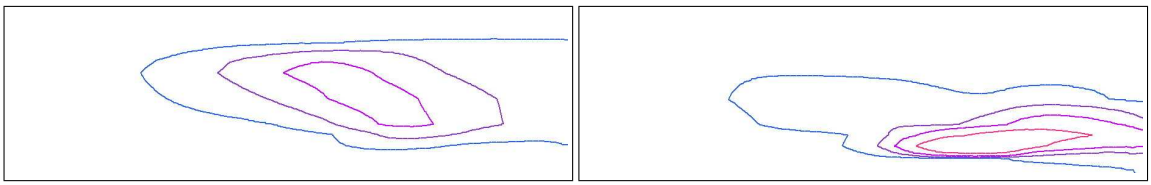

Fig. 2: *Isolines of concentration in the final time 200 years for the smallest ($dh = 10\,m$, $c = 10\,g/l$, left) and the largest ($dh = 1\,m$, $c = 50\,g/l$, right) density influence. The isoline values are (from outside) 0.1, 0.5, 1, and 2 g/l.*

On the other hand, the problem configuration and the used schemes do not allow to obtain mesh independent results. The reason can be that the influence of inhomogeneity inside the three subdomains and the changes of the numerical diffusion related to the mesh refinements amplify each other. The use of integral values also complicates the interpretation: in the bottom subdomain, there is a strong influence by escape of the mass from the domain (different in each layer of the mesh) and in the top subdomain, the value is inappropriately sensitive to the numerical approximation because it is a very small fraction of the original mass (large error relative to the local value, but smaller relative to the maximum or average value in the domain), e.g. in the case of the top layer value for $dh = 1\,\mathrm{m}$ and $c = 50\,\mathrm{g/l}$).

Here the solutions and evaluation criteria sufficient for the hydrogeological studies are not enough accurate for more exact statements on the numerical properties. We assume that an identical configuration without the internal material inhomogeneity and finer meshes in both the vertical and the horizontal directions, planned for future work, would give a better understanding of the solution behaviour.

References

[1] H.J.G. Diersch, O. Kolditz: *Variable-density flow and transport in porous media: approaches and challenges*. Adv. in Water Res. **25**, 2002, 899–944.

[2] E.O. Holzbecher: *Modeling density-driven flow in porous media: Basics, numerics, software*. Springer-Verlag Berlin and Heidelberg 1998.

[3] M. Hokr, J. Maryška, and J. Šembera: *Modelling of transport with nonequilibrium effects in dualporosity media.* In: Chen, Glowinski, Li (eds.), Current Trends in Scientific Computing, Amer. Math. Soc., 2003, 175–182.

[4] M. Hokr and V. Wasserbauer: *Velocity approximation in finite-element method for density-driven porous media flow.* In: *Sborník 3. Matematický workshop s mezinárodní účastí*, FAST VUT Brno, 2004, 49–50, full paper on CD.

[5] J. Maryška, M. Rozložník, and M. Tůma: *Mixed-hybrid finite-element approximation of the potential fluid flow problem.* J. Comput. Appl. Math. **63**, 1995, 383–392.